Debonding and Pull-Out Processes in
Fibrous Composites

Cambridge Univ. (England)

1984

19960312 100

DEPARTMENT OF DEFENSE
PLASTICS TECHNICAL EVALUATION CENTER
ARRADCOM, DOVER, N. J.   07801

DISCLAIMER NOTICE

THIS DOCUMENT IS BEST
QUALITY AVAILABLE. THE
COPY FURNISHED TO DTIC
CONTAINED A SIGNIFICANT
NUMBER OF PAGES WHICH DO
NOT REPRODUCE LEGIBLY.

BIBLIOGRAPHIC INFORMATION

Debonding and Pull-Out Processes in Fibrous Composites,

1984

by J. K. Wells, and P. W. R. Beaumont.

PERFORMER: Cambridge Univ. (England). Dept. of
            Engineering.
            CUED/C-MATS/TR-110

The processes of debonding and pull-out in fibrous
composites are described. Models predicting the debond
length and the probability distribution of pull-out lengths
of fibres and bundles are derived. These lengths are
functions of the fibre, matrix and interface properties.
Prediction is then compared with experiment and a simple
relationship between pull-out and debond lengths is found.
An understanding of the debonding and pull-out processes is
important because they affect the fracture toughness of
fibre composites.

KEYWORDS: *Fiber composites, *Failure, *Foreign technology.

Engineering
Department

DEBONDING AND PULL-OUT PROCESSES IN
FIBROUS COMPOSITES

J K Wells and P W R Beaumont

DEBONDING AND PULL-OUT PROCESSES IN
FIBROUS COMPOSITES

J K Wells* and P W R Beaumont

Cambridge University Engineering Department
Trumpington Street, Cambridge CB2 1PZ

ABSTRACT

The processes of debonding and pull-out in fibrous composites are
described. Models predicting the debond length and the probability distri-
bution of pull-out lengths of fibres and bundles are derived. These lengths
are functions of the fibre, matrix and interface properties. Prediction
is then compared with experiment and a simple relationship between pull-
out and debond lengths is found. An understanding of the debonding and
pull-out processes is important because they affect the fracture toughness
of fibre composites.

*Now at BP Research Centre, Chertsey Road, Sunbury on Thames, Middlesex

1   INTRODUCTION

The impact toughness of a fibre reinforced polymer composite is higher than that of either its constituent phases. A number of reasons have been proposed [1 - 3] based on the processes of fibre pull-out and debonding which absorb energy in the composite.

This paper analyses the fracture of a composite, enabling the pull-out and debonding lengths to be calculated. These processes can operate not only on single fibres, but also "bundles" of fibres.

2   DESCRIPTION OF THE FAILURE PROCESSES

Consider a composite of continuous fibres aligned parallel to an applied load (Fig. 1). Perpendicular to the fibre direction is a notch. Under monotonic loading the material at the notch-tip fractures and a small crack in the matrix forms. Load, once carried by the matrix, is transferred by shear to the fibres which are still intact. These shear forces eventually become so large that the bond between fibre and matrix fails. A cylindrical crack at the interface propagates from the matrix crack surface along the fibre as the applied load increases. This process is called debonding.

Some load transfer between fibre and matrix is still possible by interfacial forces due to matrix shrinkage onto the fibre during manufacture. This friction produces a non-uniform stress along the debonded fibre. Because of the variable strength of the fibre along its length the fibre is able to break some distance from the matrix crack-plane where the stress is highest. After fracture, the composite typically shows a matrix crack-plane with fibres protruding from it. This process is called Pull-Out.

3   THE PROCESS OF DEBONDING

The process of debonding is controlled by two parameters; the fibre
debond stress and the rate of increase of stress along the length of
debonded fibre due to friction.

After the matrix cracks, the fibre stress at the interfacial (debond)
crack front is the debond stress, σ_d, and the applied fibre stress when
a length x has debonded is:

$$\sigma(x) = \sigma_d + f(x) \tag{1}$$

where f(x) is the stress in the fibre caused by friction on its surface.
When $\sigma(x)$ reaches the ultimate strength of the fibre, σ_f, failure occurs
and the debond length may be determined provided σ_d and f(x) are known.

3.1   Calculation of the Debond Stress

The debond stress can be predicted using a shear-lag analysis [4 - 6].
The shear stress at the interface can be calculated as a function of applied
load, assuming debonding occurs when the shear strength of the interface
τ_o, is exceeded.   In references 4 - 6 similar results are obtained, for
example, Takaku and Arridge [6] predict:

$$\sigma_d \simeq 2\tau_o \left(\frac{E_f}{2G_m}\right)^{\frac{1}{2}} \left(\ln\left(\frac{r_m}{r_f}\right)\right)^{\frac{1}{2}} \tag{2}$$

where E_f is the Young's modulus of the fibre and G_m the matrix shear
modulus.   Other derivations also agree on the dependence of debond stress
on τ_o, E_f and G_m.   The function involving fibre radius, r_f, and the effec-
tive radius of its surrounding matrix cylinder, r_m, depends on the precise
fibre goemetry considered.

Such stress-based analyses have the disadvantage of taking no account
of any stress concentration at the crack front and may, therefore, over-

estimate the debond stress.

An alternative approach based on the energetics of failure is described by Outwater and Murphy [7] where:

$$\sigma_d = \left(\frac{4E_f G_{2c}}{r_f}\right)^{\frac{1}{2}} \qquad (3)$$

G_{2c} is the mode 2 critical strain energy release rate for interfacial cracking. Outwater and Murphy's derivation of this equation is confusing since they do not state whether the model is in the fixed grips or fixed load condition. Wells [8] rederived their model to clarify this point. Clearly, only if there is both sufficient stress to nucleate an interfacial crack and a favourable energy balance can the crack propagate.

The most convenient way of distinguishing between equations (2) and (3) is to experimentally investigate the dependence of debond stress on fibre radius. Wells [8] therefore measured the debond stress of steel wires of varying diameter embedded in epoxy resin, and the results are shown in Fig. 2. We see that the debond stress is more accurately predicted by the energy condition.

3.2   Interfacial Frictional Stress Transfer

The frictional stress transfer between fibre and matrix is due to compressive radial stresses produced both by the shrinkage of the resin during cure and thermal mismatch effects during cooling. The radial stresses can be estimated by a simple analysis developed by Harris [9] although the model does not take into account the constraining effects of surrounding fibres.

3.2.1 Simple Linear Model

If a fibre is assumed infinitely stiff, there is no Poisson contrac-

tion transverse to the direction of applied load, and the frictional inter-facial stress is uniform. The stress in a fibre embedded to a distance x is therefore:

$$\sigma(x) = \frac{2\pi r_f \tau_f x}{\pi r_f^2} = \frac{2\tau_f x}{r_f}$$

where $\tau_f = \mu P$ and μ is the coefficient of friction between fibre and matrix and P is the average radial compressive stress around the fibre. This approximation has been used extensively in the literature.

3.2.2 Non-linear Model

Although fibres are generally stiff, the simple linear model over-estimates the frictional stress transfer because Poisson contraction cannot be ignored. Full allowance for this effect is made in the derivation of Wells [8] which shows that:

$$\sigma(x) = \sigma_p (1 - \sigma^{-\beta x}) \tag{4}$$

where $\quad \sigma_p = \frac{\epsilon_o E_f}{\nu_f}, \qquad \beta = \frac{2\mu\nu_f E_m}{E_f r_f (1 + \nu_m)}$

where ν and E are the Poisson's ratio and Young's modulus of fibre and matrix (subscripts f and m respectively), μ the coefficient of friction between fibre and matrix, r_f the fibre radius and ϵ_o the 'misfit strain' between fibre and matrix. Equation (4) predicts that the rate of stress build-up will fall as the axial fibre load increases. The maximum shear stress that can be produced by frictional loading is σ_p, when the Poisson contraction of the fibre is equal to the residual strain of the matrix.

If the origin of the co-ordinates is taken as the debond crack front at which the fibre stress is σ_d, then equation (4) becomes:

$$\sigma(x) = \sigma_p - (\sigma_p - \sigma_d)e^{-\beta x} \tag{5}$$

3.3 Calculation of the Debond Length

Failure of a fibre of uniform strength occurs when the stress in that portion of fibre, between the matrix crack surfaces, reaches the strength of the fibre, σ_f. The debond crack ceases to propagate and the debonded length, ℓ_d, is therefore given by the condition:

$$\sigma_f = \sigma_p - (\sigma_p - \sigma_d) \; e^{-\frac{\beta \ell_d}{2}}$$

and hence

$$\ell_d = \frac{2}{\beta} \, \ell n \left| \frac{\sigma_p - \sigma_d}{\sigma_p - \sigma_f} \right| \tag{6}$$

where ℓ_d is the final debonded length on both sides of the matrix crack (Fig. 3). If $\sigma_d > \sigma_f$ no debonding occurs: if $\sigma_f > \sigma_p$ and $\sigma_f > \sigma_d$ debonding extends along the entire length of fibre.

3.4 Effect of Reinforcement on the Nature of Debonding

Equation (3) predicts that low stiffness or large radius fibres will have a low debond stress. Consequently, a phenomenon which may be called 'bundle debonding' can occur. This process may operate even though the fibre debond stress exceeds the fibre strength and no individual fibre debonding would be predicted. Bundles consist of a group of fibres bonded by resin. They behave as large single fibres. Such a bundle has a lower stiffness and strength than a single fibre, but with a larger radius. The interfacial parameter G_{2c}, will also be a combination of the pure matrix and interface properties.

After debonding, a bundle will have a corrugated surface, and therefore any small movement of the bundle with respect to its 'socket' will cause interlocking of these corrugations. This will produce an effective residual compressive strain on the bundle of fibres, similar to that of the single fibre case. The stress distribution and debond stress of a bundle may be approximated by equations (3) and (5) after substitution of the relevant material properties. These corrugations may also provide an air-gap which accounts for the whitening observed in debonded glass fibre composites. A debonded single fibre would not produce a sufficiently large airgap to create such whitening effects.

3.4.1 Calculation of Bundle Properties for Calculation of Bundle Debond Length

The bundle stiffness and strength may be calculated using the rule-of-mixtures where the fracture of weak fibres reduces the strength of the bundle to 80% of the ideal rule-of-mixtures prediction [10]. Poisson's ratio of a bundle is that of a typical composite of appropriate fibre volume fraction ($\nu = 0.32$).

The interface parameter, G_{2c}, is assumed to be a linear function of the two constituent material properties:

$$G_{2c} = \frac{1}{a} \left| \pi r_f G_1 + (a - 2r_f) G_2 \right| \tag{7}$$

where G_1 and G_2 are the critical energy release rates for fracture of interface and pure resin respectively. The spacing between fibres centres around the edge of the bundle, a, is given by the square packing approximation:

$$a = \left(\frac{\pi r_f^2}{V_f} \right)^{\frac{1}{2}} \tag{8}$$

where V_f is the volume fraction of fibres in the bundle.

Wells [8] measured $G_2 \simeq 500$ Jm^{-2} for an epoxy resin matrix and G_1 approximately 50, 2 and 60 Jm^{-2} for E-glass, Kevlar and high strength carbon fibres in epoxy respectively. The misfit strain between bundle and matrix was found to be about 5%, and the radius of a bundle, r_b, was typically 500 µm.

3.5 Comparison of Observed and Predicted Debond Lengths in Model Composites

Experiments have been carried out on model composite specimens where debond lengths may be accurately measured and compared to theoretical predictions. The specimens have been described previously [3]. Briefly, a specimen consisted of a single layer of glass reinforcing tows close to the tensile side of a small epoxy beam loaded in three point bending.

TABLE 1: Variation in Debond Lengths with Specimen Type

SPECIMEN TYPE	No. OF SPECIMENS	DEBOND LENGTH (mm)		NOTE
		OBSERVED	PREDICTED	
A	30	2.7 ± 0.2	3.9	V_f = 23%
				r_b = 0.5 mm
B	90	5.8 ± 0.6	7.9	V_f = 40%
				r_b = 0.45 mm
C	10	7.1 ± 1.0	8.7	As B with
				G_1 = 0

The observed lengths of bundle debonding are shown in Table 1 each result being the average of at least 100 measurements (10 measurements per specimen). Results for specimens of three types are presented:

(i)   Type A had no weft fibres holding the main tows in place, enabling

bundle spreading to occur during manufacture.

(ii) Type B had a small number of light weft fibres present, holding the bundle together and reducing the inter-fibre spacing. This corresponds to a composite with a locally higher volume fraction.

(iii) Type C were specimens prepared as type B, but the fibres were sprayed with mould release fluid, producing a weak fibre/matrix bond.

Table 1 also shows the predicted debond lengths using equations (3), (6), (7) and (8), with substitution of material properties listed in Table 2.

TABLE 2: Properties of Fibres and Epoxy Resin

| | | FIBRE | | RESIN |
		GLASS	CARBON	
Strength	(MPa)	1650	2480	80
Young's Modulus	(GPa)	70	230	3
Radius	(μm)	7	4	-
Poisson's Ratio		0.2	0.2	0.35

Values of G_1, G_2 and misfit strain, ε_o, are those reported in the previous section, except in the case of type C specimens where it is assumed that no fibre-matrix bonding occurred and consequently $G_1 = 0$ in this case. Agreement between observed and predicted values is generally good although the predictions are typically 30% higher than the observed value.

4   THE PROCESS OF PULL-OUT

The fundamental origin of pull-out is the variable strength of the reinforcing fibre. In the absence of strength-reducing flaws a fibre

would break in the region of maximum stress (i.e. between the faces of a matrix crack), and no pull-out would result. However, when a brittle fibre carries a non-uniform load along its length the fibre may either fracture at a large flaw in a region of low stress or at a minor flaw at a point of higher stress. This is shown schematically in Fig. 4. In this case fibre fracture will occur at point 'A' away from the region of maximum stress and produce pull-out during crack propagation.

4.1   A Statistical Model for Pull-Out

After the matrix cracks, the load on a fibre close to the crack tip increases causing debonding. Friction between fibre and matrix gives rise to a non-uniform stress distribution along the fibre length.

The variable strength of a brittle fibre is controlled by the distribution of flaws along its length. Experiments show that the strength of such material is well described by a Weibull distribution. On loading the material up to a stress σ, a fraction of the fibres $P(\sigma)$ will fail; in its simplest form:

$$P(\sigma) = 1 - e^{(-(\sigma/\sigma_o)^m)} \tag{9}$$

where σ_o is a characteristic strength and m the Weibull modulus.

Consider a debonded fibre with a series of sections of length δx to be non-uniformly loaded, Fig. 5. The stress in the ith section increases from zero to σ_i as the debond crack propagates along the fibre. The nth section is at the point of maximum fibre stress, i.e. in the plane of the matrix crack. The probability of failure in loading section i from zero load to σ_i is given by the cumulative probability of failure $P(\sigma_i)$.

However, the probability of failure occurring in the ith segment is not simply $P(\sigma_i)$. It also depends upon the probability that a more highly stressed section has not broken before the flaw in the ith section

causes failure of the fibre. This is given by the sum of $1 - P(\sigma_j)$ for all $j > i$, i.e. all sections more highly loaded than section i*.

The relative probability of fracture occurring in section i is therefore given by:

$$f_i \propto P(\sigma_i) \sum_{j=i+1}^{n} (1 - P(\sigma_j)) \, \delta x \qquad (10)$$

Equation (10) may be re-expressed to present an integral form of the cumulative probability function:

$$F(x) = \frac{\int_0^x P(\sigma(x')) \left\{ \int_{x'}^{\ell_d/2} 1 - P(\sigma(x'')) \, dx'' \right\} dx'}{\int_0^{\ell_d/2} P(\sigma(x')) \left\{ \int_{x'}^{\ell_d/2} 1 - P(\sigma(x'')) \, dx'' \right\} dx'} \qquad (11)$$

The pull-out length is given by:

$$\ell_p = \frac{\ell_d}{2} - x$$

and $F(x')$ is the cumulative probability of x being less than x'. Consequently the cumulative probability distribution of the pull-out length being less than or equal to ℓ_p is:

$$1 - F\left(\frac{\ell_d}{2} - \ell_p\right)$$

The model assumes that the entire flaw spectrum is repeated in a length of fibre which is small by comparison with the pull-out length. This is justified since the average strength of the fibres changes only slowly with increasing gauge length. It implies that the full range of flaws must be present in short lengths of fibre.

---

*An allowance for the probability of a severe flaw causing fracture in a section under lower stress, before fibre failure occurs in section i, is made by the use of the cumulative Weibull distribution, $P(\sigma)$.

4.2   The Effect of the Reinforcement on the Nature of Pull-Out

For certain composites the debonding of single fibres does not occur because the debond stress is greater than the fibre strength. This behaviour is anticipated in materials with a strong fibre/matrix bond or high fibre stiffness, as found in carbon fibre reinforced systems. In such cases the pull-out of individual fibres is not possible, but instead a bundle of fibres (which debonds more easily than the individual fibres) behaves as a large fibre. Although a composite, the bundle still has a variable strength which can be described by a Weibull distribution with a Weibull modulus about 3.5 times larger than the single fibre and a strength of about 80% of the rule-of-mixute prediction [Harlow and Pheonix, 10]. The stress distribution in the bundle is similar to that in the single fibre (Section 3).

The nature of the pull-out process is therefore controlled by the debonding process. If fibres can debond, they will pull-out individually. Glass and Kevlar* should normally do this. However, if only the bundle debonds then the bundle will fracture away from the matrix crack plane and pull-out as a small piece of intact composite; this is what CFRP is predicted to do. The process may be analysed using equation (11) when the appropriate substitutions are made. In general, a composite may show a combination of the two types of pullout.

4.2.1   Fractographic Observations of Pull-Out

Fractured samples of epoxy containing E-glass, Kevlar 49 and carbon

---

*Although Kevlar is a polymeric fibre, it appears to behave as a brittle material. In the absence of any detailed information, the Weibull distri-bution (with a Weibull modulus equal to that of glass and carbon) is used to characterise the fibre strength.

(Grafil EX-AS) have been examined in a scanning electron microscope (SEM) in order to verify the above predictions. Figure 6 shows the fracture surface of a unidirectional or [0/90]$_s$ laminate. Glass and Kevlar show individual fibre pull-out with little or no matrix between the fibres. By contrast, the carbon fibre reinforced epoxy shows a solid bundle which has fractured and pulled-out with intact matrix binding the fibres. These observations are in agreement with the debonding behaviour predicted in Section 4.2, although variations in the properties of the fibre/matrix bond could allow the other mode of pull-out to occur.

4.3 Comparison of Predicted and Observed Distributions in Composites

For a typical composite with brittle fibre reinforcement the function P(σ) is of the Weibull form (eqn. 9) and for a debonded fibre the stress distribution is:

$$\sigma(x) = \sigma_p - (\sigma_p - \sigma_d) \, e^{-\beta x}$$

The integral (equation 11) has been evaluated numerically for various materials and the predictions compared with experiment.

4.3.1 Results for GFRP

Beaumont and Anstice [11] measured a large number of pull-out lengths in GFRP in an effort to ascertain their distribution. The pull-out lengths were well described by a Weibull distribution but of a much lower modulus than for the fibre strength distribution. The average of the Weibull parameters from over 2000 measurements of pull-out lengths are:

$$\bar{\ell}_o = 0.24 \pm 0.08 \text{ mm}$$

$$\bar{m} = 2.2 \pm 0.42$$

This distribution is shown in Fig. 7 and is compared with the prediction

of eqn. (11), using typical E-glass/epoxy properties listed in Table 2.
Good agreement is found between the predicted and experimental distributions
except at small pull-out lengths. The model predicts that the most probable
pull-out length (the point at which the slope is maximised) is at $\ell_p = 0$,
which is intuitively correct since the stress is maximised at that point.
By comparison, the Weibull distribution predicts zero probability of zero
length pull-outs.

4.3.2 Results for CFRP

The procedure described in Section 4.3.1 has been applied to bundle
pull-out of high strength carbon fibres using data from Wells [8]. Charac-
teristic Weibull parameters for 500 measurements were:

$$\bar{\ell}_o = 0.47 \pm 0.03 \text{ mm}$$

$$\bar{m} = 1.9 \pm 0.1$$

This distribution is shown in Fig. 8, and may be compared with the result
from eqn. (11) using typical values for carbon fibre in epoxy (see Table 2)
and a bundle misfit strain of 3%. The main differences in shape of the
distributions, noted in Section 4.3.1, are evident although agreement
between average values is good.

4.4   A Method for the Rapid Calculation of Pull-Out Lengths

So far the theory has successfully predicted the shape and position
of the cumulative probability distributions for both individual fibre
and bundle pull-out cases. However, calculations of the complete proba-
bility distribution is time-consuming and often an average value of the
pull-out length is all that is required. Consequently the effect of chang-
ing composite properties on the shape and position of the distribution
has been investigated and correlations between pull-out and debond lengths

- 13 -

have been sought as a means of convenient prediction.

4.4.1 Effect of Varying Material Properties on Pull-Out Distributions

From eqn. (11), the pull-out length distribution is affected by any parameters which reflect changes in the flaw or stress distributions in the fibre. Changes in most of these parameters will also affect the debond length. Figure 9 shows the effect of varying fibre misfit strain, Weibull modulus, fibre strength and radius on the probability distribution, using values which are otherwise typical of an E-glass/epoxy composite. In particular, it should be noted that the distribution is relatively insensitive to the Weibull modulus.

4.4.2 Correlation between Fibre Pull-out and Fibre Debond Length

Figure 10 shows the relationship between the average pull-out length, $\bar{\ell}_p$, and the fibre debond length, ℓ_d (as calculated using eqn. 6) when several parameters vary. The average pull-out length for both glass and Kevlar reinforced material may be estimated by:

$$\bar{\ell}_p = \frac{\ell_d}{6.8}$$

This approximation is accurate to within ± 10% for $\bar{\ell}_p$ < 0.3 mm (or $\bar{\ell}_d$ < 2.1 mm). The behaviour due to changing G_1, and therefore the debond stress, is least well predicted.

4.4.3 Correlation between Bundle Pull-Out and Bundle Debond Length

Figure 11 shows a similar variation between pull-out and debond lengths for typical high strength carbon fibre composite. There is a correlation between ℓ_p and ℓ_d for changes of fibre strength, radius and fibre misfit strain. However, as noted in the previous section, changes

due to variations in debond stress do not follow the same trend. Neverthe-
less, an approximate relationship may be found in the region 0.22 mm <
$\bar{\ell}_p$ < 0.32 mm (7.5 mm < ℓ_d < 12 mm) to an accuracy of ± 20%, namely:

$$\bar{\ell}_p = \frac{\ell_d}{35} \tag{12}$$

5 SUMMARY

The energy absorption in composites is dependent on the length
of debonding and pull-out. These processes have been studied to enable
the lengths to be calculated from fibre, resin and interface properties.

The study shows that two types of debonding are possible, namely
single fibre and bundle debonding. Debond lengths have been measured
and found to be in agreement with the predictions of the theory.

A model has been proposed for the fracture of brittle fibres under
non-uniform stress, predicting the probability of fracture sites. As
a result of the two types of debonding (single fibre and bundle), two
corresponding modes of pull-out have been proposed and observed in practice.

References

1   Kelly, A, Proc. Roy. Soc. Lond. A282 (1964) 63

2   Kaelble, D H, J. Adhesion, 5 (1973), 245

3   Kirk, J N, Munro, M and Beaumont, P W R, J. Mater. Sci., 13, (1978) 2197

4   Greszczuk, L B, ASTM STP 452 (1969), 42

5   Lawrence, P J, J. Mater. Sci., 7 (1972), 1

6   Takaku, A and Arridge, R G C, J. Phys. D: Appl. Phys., 6, (1973), 2038

7   Outwater, J D and Murphy, M C, Paper 11c, 24th Annual Technical Conference of Composites Section SPI (1969)

8   Wells, J K, PhD dissertation, Cambridge University, September 1982

9   Harris, B, J. Mater. Sci., 13 (1978), 173

10   Harlow, D G and Pheonix, S L, J. Comp. Mater., 12 (1978), 195

11   Beaumont, P W R and Anstice, P D, J. Mater. Sci., 15 (1980), 2619

Figure Captions

1   Schematic of composite fracture ahead of a notch.

2   Variation of debond stress with wire radius.

       Solid line; debond
       stress calculated from equation 3 with E_f = 210 GPa, and G_{2c} = 200 Jm^{-2}.

       Dashed line; debond stress from equation 2 with G_m = 1.1 GPa,
       τ_o = 20 MPa, r_m = 10 mm.

3   Calculation of the debond length

4   Schematic showing origin of pull-out

5   Schematic of debonded fibre

6   Pull-out in (a) glass, (b) Kevlar and (c) carbon fibre reinforced
       plastic

7   Predicted and best-fit Weibull distributions for fibre pull-out
       lengths in GFRP. ε_o = 0.75%.

8   Predicted and best-fit Weibull distributions for bundle pull-out
       lengths in CFRP. ε_b = 3%.

9   Effect of changing material parameters on fibre pull-out distribution
       in GFRP. Parameter varying: (a) misfit strain, (b) Weibull modulus,
       (c) fibre strength, and (d) fibre radius.

10   Correlations between fibre pull-out and debond lengths for (a) glass,
       and (b) Kevlar reinforced material.

       (Parameter varied $\bullet$, σ_f; +, ε_o; $\times$, r_f; and $\blacktriangle$, G_1)

11   Predicted correlation between bundle pull-out and debond lengths
       for high strength carbon fibre composite (see figure 10 for key)
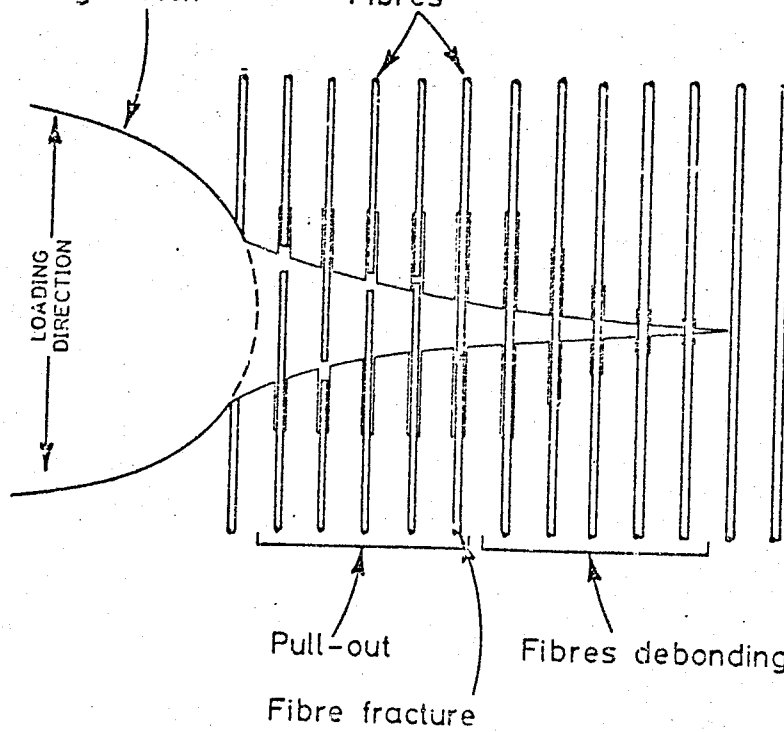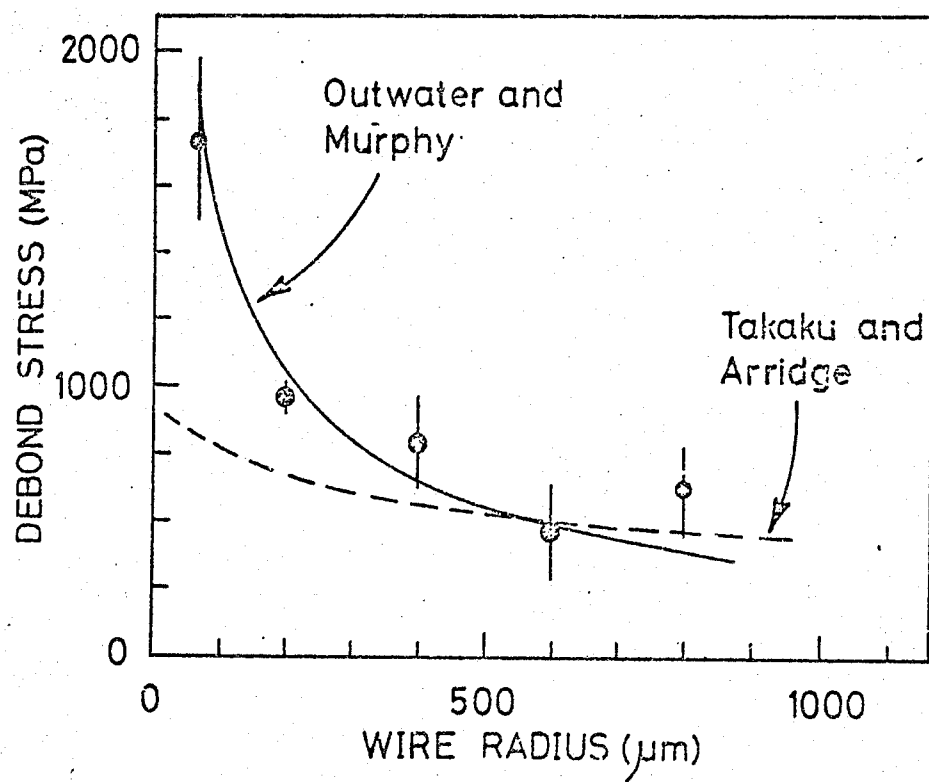
Pre-existing notch

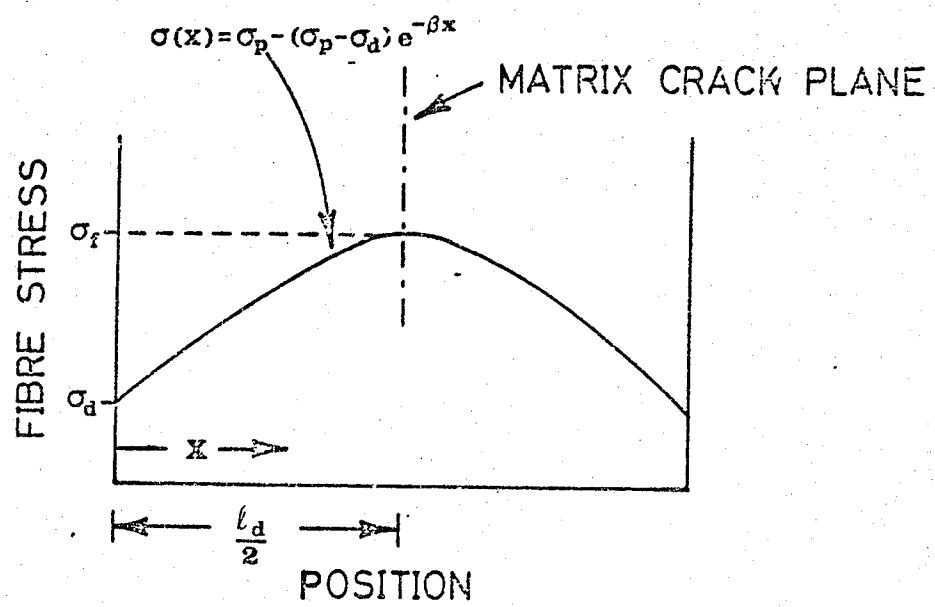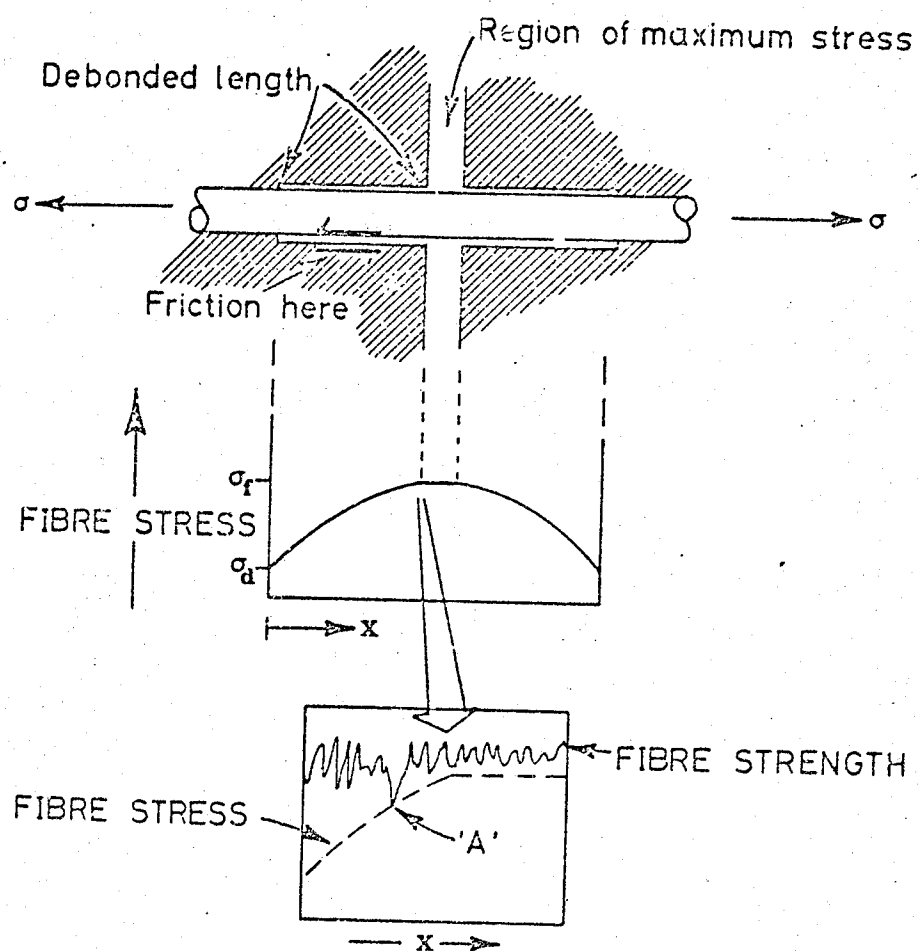Fibres

LOADING DIRECTION

Pull-out

Fibre fracture

Fibres debonding

$$\sigma(x) = \sigma_p - (\sigma_p - \sigma_d)\, e^{-\beta x}$$

MATRIX CRACK PLANE

FIBRE STRESS

σ_ℓ

σ_d

$x \longrightarrow$

$\dfrac{\ell_d}{2}$

POSITION

Region of maximum stress

Debonded length

$\sigma \longleftarrow$ $\longrightarrow \sigma$

Friction here

FIBRE STRESS

σ_f

σ_d

$\longrightarrow x$

FIBRE STRESS

FIBRE STRENGTH

'A'

$\longrightarrow x \longrightarrow$

δx

| 1 | 2 | 3 | | i | | n | |

$0 =$

$x = x_3$

$x = x_n = \dfrac{l_d}{2}$

GLASS

CUMULATIVE PROBABILITY

Theory

Average best-fit Weibull distribution to data

PULL-OUT LENGTH (mm)

CARBON

Theory →

Average best-fit Weibull
distribution to data

CUMULATIVE PROBABILITY

PULL-OUT LENGTH (mm)

GLASS

$\bar{l}_p = l_d / 6.8$